Eur. Phys. J. D (2021) 75:45
https://doi.org/10.1140/epjd/s10053-021-00043-5

THE EUROPEAN PHYSICAL JOURNAL D

Regular Article - Atomic Physics

Electron-impact ionization of the Pb atom

M. S. Pindzola[1,a], S. D. Loch[1], and J. P. Colgan[2]

[1] Department of Physics, Auburn University, Auburn, AL, USA
[2] Theoretical Division, Los Alamos National Laboratory, Los Alamos, NM, USA

Received 19 November 2020 / Accepted 4 January 2021 / Published online 8 February 2021

Abstract. Electron-impact ionization cross sections are calculated for the ground configuration of the Pb atom. Time-dependent close-coupling cross sections for the direct ionization of the $6s$ and $6p$ subshells leading to single ionization are calculated with and without a polarization potential. Configuration-average distorted-wave cross sections for the direct ionization of the $6s$ and $6p$ subshells leading to single ionization are also calculated with and without a polarization potential. We find the time-dependent close-coupling cross sections using a polarization potential to be in good agreement with convergent-close-coupling cross sections using a polarization potential. The total direct ionization cross sections are compared to two sets of experimental measurements. The differences between the direct ionization cross sections and the experimental measurements are mainly due to indirect ionization cross sections coming from the $6s^2 6p^2 \rightarrow 6s6p^3$ excitation followed by autoionization.

1 Introduction

Electron-impact ionization cross sections for heavy metal atoms are needed for the accurate modelling of astrophysical and fusion plasmas. Lead has the highest cosmic abundance among the elements heavier than Barium [1]. Lead–Lithium alloys are also candidates for liquid breeders in fusion blanket systems [2]. Heavy neutral atoms such as Pb are also very challenging for theoretical methods to produce accurate electron-impact direct and indirect ionization cross sections. Perturbative methods are generally found to over-estimate the ionization cross sections from neutral atoms, although become more accurate as the charge of the target ion increases [3].

Recently the configuration-average distorted-wave and time-dependent close-coupling methods were used to calculate direct ionization cross sections for both W [4] and W^+ [5]. The close-coupling calculations for neutral W were found to be 15% lower for the $6s^2$ subshell and 44% lower for the $5d^4$ subshell when compared to the distorted-wave calculations.

In this paper we carry out configuration-average distorted-wave and time-dependent close-coupling calculations with and without a polarization potential for the direct ionization of the $6p^2$ and $6s^2$ subshells for Pb. The largest contribution to the indirect ionization cross section for Pb comes from the $6s^2 6p^2 \rightarrow 6s6p^3$ transition. Due to its complexity we leave its cross section to future large scale R-matrix pseudo-state calculations. We note that direct ionization cross sections were calculated for Pb using the binary-encounter-Bethe approximation and that indirect ionization cross sections were calculated for Pb using the scaled plane-wave Born approximation, but the cross sections were said to be unreliable [6]. Recently direct ionization cross sections were calculated for Pb using the convergent close-coupling method [7] with a polarization potential and indirect ionization cross sections were calculated for Pb using the R-matrix B-spline method [7]. We also note that four sets of crossed-beams measurements have been made for the electron ionization of Pb [8–11]. In this paper we investigate whether the use of a polarization potential lowers the calculated direct ionization cross sections for Pb, both to produce accurate Pb direct ionization cross sections and as a guide to the importance of polarization potentials in future ionization calculations of heavy elements.

The rest of this paper is organized as follows. In Sect. 2 we give a brief review of the configuration-average distorted-wave and time-dependent close-coupling methods used to calculate electron-impact ionization cross sections. In Sect. 3 we present our cross section results for the electron-impact ionization of the Pb atom. We conclude with a brief summary and future plans in Sect. 4. Unless otherwise stated, we will use atomic units.

2 Theory

The perturbative configuration-average distorted-wave (CADW) cross section is given by [12]:

[a] e-mail: pindzola@physics.auburn.edu (corresponding author)

$$\sigma_{ion}(n_0 l_0) = \frac{32 w_0}{k_i^3} \int_0^{E/2} \frac{d(k_e^2/2)}{k_e k_f} \times \sum_{l_i l_e l_f} (2l_i + 1)(2l_e + 1) (2l_f + 1) S(n_0 l_0 k_i l_i \rightarrow k_e l_e k_f l_f) \ , \quad (1)$$

where $S(n_0 l_0 k_i l_i \rightarrow k_e l_e k_f l_f)$ is the first-order perturbation theory partial scattering probability. The bound and continuum orbitals are calculated in the Hartree–Fock relativistic (HFR) approximation [13]. A variable radial mesh is employed to fully resolve all of the orbitals of the Pb atom.

The non-perturbative time-dependent close-coupling (TDCC) cross section is given by [14]:

$$\sigma_{ion}(n_0 l_0) = \frac{\pi w_0}{8(2l_0 + 1)E} \times \sum_{LS} (2L + 1)(2S + 1) P(n_0 l_0 LS) \ , \quad (2)$$

where $P(n_0 l_0 LS)$ is the non-perturbative theory partial ionization probability. This probability is obtained by propagating the time-dependent close-coupling equations until convergence for each partial wave is obtained [14]. The time-dependent close-coupled equations are obtained from a Hamiltonian that includes direct and local exchange potential terms as well as the usual kinetic energy term [14].

For both the CADW and TDCC cross section calculations we use a polarization potential given by:

$$V_{pol}(r) = -\frac{\alpha}{2r^4}(1.0 - \exp(-r/r_c)^6) \ , \quad (3)$$

where $\alpha = 47.0$ and $r_c = 3.45689$ for Pb [15]. A polarization potential accounts for the incoming electron polarizing the target electron charge cloud.

3 Results

3.1 Direct ionization of the 6*p* subshell

CADW calculations were made for direct ionization of the 6*p* subshell of Pb using Eq. (1) with no polarization potential. TDCC calculations for direct ionization of the 6*p* subshell of Pb using Eq. (2) with no polarization potential were made on a 1344 × 1344 point lattice with a variable mesh spacing of $\delta r = 0.001$ to $\delta r = 0.200$ ranging from $r = 0.0$ to $r = 91.5936$ for both sets of points. CADW calculations were used to topup the TDCC calculations for $l = 8 - 50$.

Both CADW and TDCC direct ionization cross sections for the 6*p* subshell of Pb are presented in Fig. 1. We use simple analytical formulae to smoothly join the 4 calculated TDCC cross sections and to extend the results to higher energies. We also compare the CADW and TDCC cross sections with recent calculations made using the convergent close-coupling method [7] with a polarization potential, noting that all of the results with no polarization potential are higher than the convergent close-coupling results with the inclusion of a polarization potential.

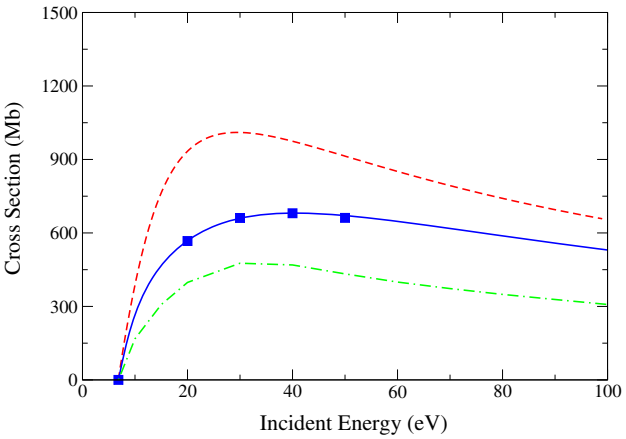

Fig. 1 Electron-impact direct ionization of the 6*p* subshell of Pb. Dashed line (red): distorted-wave method, solid line with squares (blue): time-dependent close-coupling method, dot-dash line (green): convergent close-coupling method [7] with a polarization potential (1.0 Mb = 1.0×10^{-18} cm^2)

CADW calculations were made for direct ionization of the 6*p* subshell of Pb using Eq. (1) with the polarization potential of Eq. (3). TDCC calculations for direct ionization of the 6*p* subshell of Pb using Eq. (2) with the polarization potential of Eq. (3) were made on a 1344 × 1344 point lattice with the same variable mesh as used before. CADW calculations were used to topup the TDCC calculations for $l = 8 - 50$.

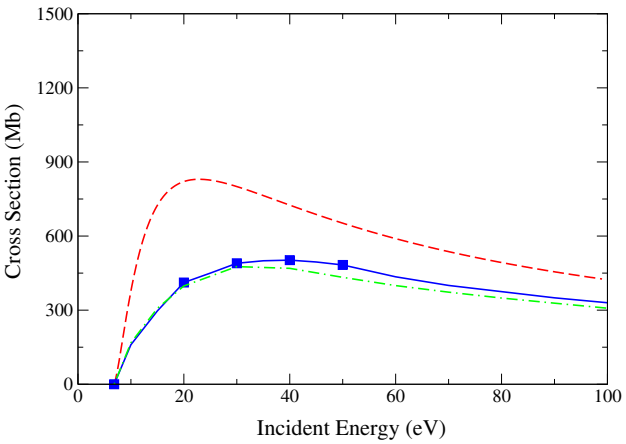

Fig. 2 Electron-impact direct ionization of the 6*p* subshell of Pb. Dashed line (red): distorted-wave method with a polarization potential, solid line with squares (blue): time-dependent close-coupling method with a polarization potential, dot-dash line (green): convergent close-coupling method [7] with a polarization potential (1.0 Mb = 1.0×10^{-18} cm^2)

Both CADW and TDCC direct ionization cross sections for the 6p subshell of Pb are presented in Fig. 2. We use simple analytical formulae to smoothly join the 4 calculated TDCC cross sections and to extend the results to higher energies. We also compare the CADW and TDCC cross sections with recent calculations made using the convergent close-coupling method [7] with a polarization potential. Good agreement is found between the non-perturbative TDCC results with a polarization potential and the non-perturbative convergent close-coupling results with a polarization potential.

3.2 Direct ionization of the 6s subshell

CADW calculations were made for direct ionization of the 6s subshell of Pb using Eq. (1) with no polarization potential. TDCC calculations for direct ionization of the 6s subshell of Pb using Eq. (2) with no polarization potential were again made on a 1344×1344 point lattice with the same variable mesh as used before for the 6p subshell. CADW calculations were used to topup the TDCC calculations for $l = 8 - 50$.

Both CADW and TDCC direct ionization cross sections for the 6s subshell of Pb are presented in Fig. 3. We again use simple analytical formulae to smoothly join the 4 calculated TDCC cross sections and to extend the results to higher energies. We also compare the CADW and TDCC cross sections with recent calculations made using the convergent close-coupling method [7] with a polarization potential.

CADW calculations were made for direct ionization of the 6s subshell of Pb using Eq. (1) with the polarization potential of Eq. (3). TDCC calculations for direct ionization of the 6s subshell of Pb using Eq. (2) with the polarization potential of Eq. (3) were made again on a 1344×1344 point lattice with the same variable mesh as used before. CADW calculations were used to topup the TDCC calculations for $l = 8 - 50$.

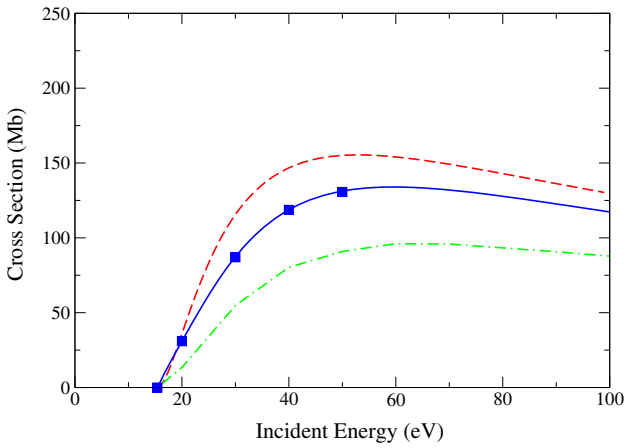

Fig. 3 Electron-impact direct ionization of the 6s subshell of Pb. Dashed line (red): distorted-wave method, solid line with squares (blue): time-dependent close-coupling method, dot-dash line (green): convergent close-coupling method [7] with a polarization potential (1.0 Mb = 1.0×10^{-18} cm^2)

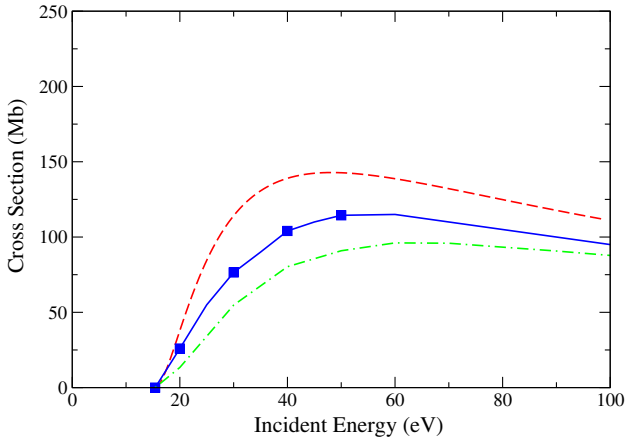

Fig. 4 Electron-impact direct ionization of the 6s subshell of Pb. Dashed line (red): distorted-wave method with a polarization potential, solid line with squares (blue): time-dependent close-coupling method with a polarization potential, dot-dash line (green): convergent close-coupling method [7] with a polarization potential (1.0 Mb = 1.0×10^{-18} cm^2)

Both CADW and TDCC direct ionization cross sections for the 6s subshell of Pb are presented in Fig. 4. We again use simple analytical formulae to smoothly join the 4 calculated TDCC cross sections and to extend the results to higher energies. We also compare the CADW and TDCC cross sections with recent calculations made using the convergent close-coupling method [7] with a polarization potential. The same pattern as with the 6p ionization is found, with the use of a polarization potential in the TDCC calculation bringing the TDCC cross section into closer agreement with the convergent close-coupling results with a polarization potential, in this case with the TDCC cross section being slightly higher than the convergent close-coupling results.

3.3 Comparison with experiment

The total TDCC direct ionization cross sections for the 6p and 6s subshells of Pb using a polarization potential are compared with the crossed-beams measurements [10,11] in Fig. 5. The inclusion of the polarization potential in the TDCC calculations lowers the direct ionization significantly, by around 30%. The incoming electron polarizes the charge cloud of the target atom. For a heavy target atom such as Pb, with relatively diffuse valence orbitals, this polarization effect can be significant, especially at the relatively low impact energies where the ionization cross section is at a maximum. The TDCC direct ionization cross sections fall below the crossed-beams measurements of Freund et al. [10] and of McCartney et al. [11]. The convergent close-coupling direct ionization cross sections for the 6p and 6s subshells of Pb using a polarization potential are in

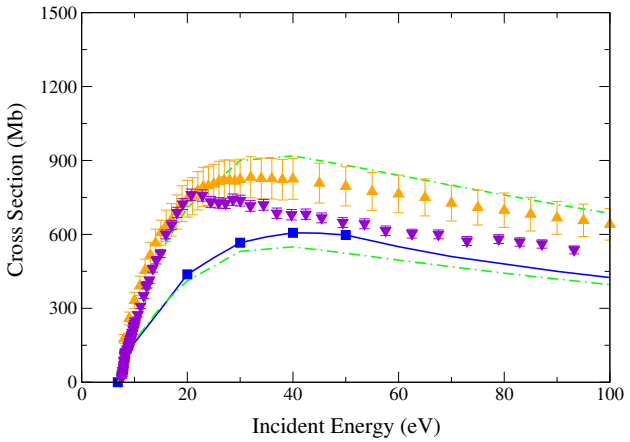

Fig. 5 Electron-impact ionization of Pb. Solid line with squares (blue): total TDCC direct ionization cross section with a polarization potential, dot-dash line (green): total CCC direct ionization cross section [7] with a polarization potential, dot-dash-dash line (green): total CCC direct ionization cross section with a polarization potential plus R-matrix B-spline indirect ionization cross section [7], up triangles (orange): crossed-beams measurements [10]. down triangles (violet): crossed-beams measurements [11] (1.0 Mb = 1.0×10^{-18} cm^2)

good agreement with the total TDCC direct ionization cross sections for the $6p$ and $6s$ subshells of Pb using a polarization potential and also fall below the crossed-beams measurements [10,11]. We also compare the convergent close-coupling direct ionization cross sections for the $6p$ and $6s$ subshells added to R-matrix B-spline indirect ionization cross sections and find good agreement with the crossed-beams measurements of Freund et al. [10] as earlier reported [7]. Thus, the difference between the TDCC total direct ionization cross section results and the experiment is likely due to this excitation-autoionization contribution.

4 Summary

Electron-impact ionization cross sections for the single ionization of the neutral Pb atom have been presented. Configuration-average distorted-wave, time-dependent close-coupling, and convergent close-coupling [7] cross sections were compared for the direct ionization of the $6p$ and $6s$ subshells of the Pb atom. The total direct ionization cross sections for the TDCC and CCC methods were then compared with two sets of crossed-beams measurements [10,11].

In the future we plan to complete R-matrix calculations for the indirect ionization cross section of Pb to compare directly with R-matrix B-spline calculations [7]. We also hope with future TDCC calculations on a variety of numerical lattices to better understand the differences with the convergent close-coupling calculations [7].

This work was supported in part by grants from the US Department of Energy. Computational work was carried out at the National Energy Research Scientific Computing Center (NERSC). A portion of this work was supported by the US Department of Energy through the Los Alamos National Laboratory. Los Alamos National Laboratory is operated by Triad National Security, LLC, for the National Nuclear Security Administration of the US Department of Energy (Contract No. 89233218NCA000001).

Author contributions

All authors contributed in the preparation of the manuscript.

Data availability statement This manuscript has no associated data, or the data will not be deposited. [Authors' comment: Any data can be obtained directly from the first author.]

References

1. A. Alonso-Medina, Spectrochim. Acta Part B **63**, 598 (2008)
2. M. Kondo, Y. Nakajima, Fusion Eng. Des. **88**, 2556 (2013)
3. D.C. Griffin, C.P. Ballance, M.S. Pindzola, F. Robicheaux, S.D. Loch, J.A. Ludlow, M.C. Witthoeft, J. Colgan, C.J. Fontes, D.R. Schultz, J. Phys. B **38**, L199 (2005)
4. M.S. Pindzola, S.D. Loch, A.R. Foster, J. Phys. B **50**, 095201 (2017)
5. M.S. Pindzola, S.D. Loch, J. Phys. D **73**, 78 (2019)
6. Y.K. Kim, P.M. Stone, J. Phys. B **40**, 1597 (2007)
7. M.P. van Eck, D.V. Fursa, I. Bray, O. Zatsarinny, K. Bartschat, J. Phys. B **53**, 015204 (2020)
8. I. Pavlov, S.I. Stotskii, Sov. Phys. JETP **31**, 61 (1970)
9. D.G. Golovach, A.N. Drozdov, V.I. Rakhovskii, V.M. Shustryakov, Meas. Tech. USSR **30**, 587 (1987)
10. R.S. Freund, R.C. Wetzel, R.J. Shul, T.R. Hayes, Phys. Rev. A **41**, 3575 (1990)
11. P.C.E. McCartney, M.B. Shah, J. Geddes, H.B. Gilbody, J. Phys. B **31**, 4821 (1998)

12. M.S. Pindzola, C.P. Ballance, J.A. Ludlow, S.D. Loch, D.C. Griffin, J. Phys. B **43**, 025201 (2010)
13. R.D. Cowan, *The Theory of Atomic Structure and Spectra* (University of California Press, California, 1981)
14. M.S. Pindzola, F. Robicheaux, S.D. Loch, J.C. Berengut, J.P. Colgan, M. Foster, D.C. Griffin, C.P. Ballance, D.R. Schultz, T. Minami, N.R. Badnell, M.C. Witthoeft, D.R. Plante, D.M. Mitnik, J.A. Ludlow, U. Kleiman, J. Phys. B **40**, R39 (2007)
15. P. Schwerdtfeger, J.K. Nagle, Mol. Phys. **117**(9–12), 1200 (2019)